Supporting Information

Ternary $Pb_{1-x}Cd_xS$ Quantum Dot-Based UV-vis-NIR Photoelectrochemical Photodetection with Superior Photoresponsivity and Detectivity

Youhua Zhu,‡[a] Zhihui Huang,‡[ab] Songrui Wei,‡[c] Yi Hu,[b] Hongyan Chen,[b] Mengke Wang,[b] You Zi*[b] and Weichun Huang*[b]

[a]School of Microelectronics and School of Integrated Circuits, Nantong University, Nantong 226019, P. R. China

[b]School of Chemistry and Chemical Engineering, Nantong University, Nantong 226019, Jiangsu, P. R. China

[c]Key Laboratory of Optoelectronic Devices and Systems of Ministry of Education and Guangdong Province, College of Physics and Optoelectronic Engineering, Shenzhen University, Shenzhen 518060, P. R. China

‡These authors contributed equally to this work.

Table S1 The elemental contents of $Pb_{1-x}Cd_xS$ QDs with different x obtained from the EDS elemental mapping.

Samples	Pb (mol%)	Cd (mol%)	S (mol%)
PbS QDs	48.3	0	51.7
$Pb_{0.25}Cd_{0.75}S$ QDs	9.8	44.4	45.8
$Pb_{0.50}Cd_{0.50}S$ QDs	27.1	24.7	48.2
$Pb_{0.75}Cd_{0.25}S$ QDs	34.3	11.5	54.2
CdS QDs	0	47.7	52.3

Table S2 Laser power density (P_λ) of incident light with various irradiation wavelengths.

Laser	P_λ (mW cm^{-2})			
	Level I	Level II	Level III	Level IV
Simulated light (SL)	21.8	47.7	171	272
380 nm	0.15	0.30	0.85	1.50
420 nm	0.40	0.60	1.90	3.10
450 nm	2.95	6.65	21.7	38.0
475 nm	2.87	5.95	22.4	39.3
520 nm	3.20	7.15	23.2	40.2
600 nm	3.05	6.30	20.2	35.1
700 nm	4.72	10.3	33.1	57.4
808 nm	2.42	5.15	16.5	28.4
940 nm	1.23	2.25	3.61	4.58

Table S3 Photocurrent density (unit: μA cm^{-2}) of the as-fabricated $Pb_{0.50}Cd_{0.50}S$ QDs under SL and lasers with different wavenumbers at 0.4 V in 0.1 M KOH.

Pb_2Cd_2S QDs	Level I	Level II	Level III	Level IV
SL	8.031	28.22	74.14	**80.92**
380 nm	4.096	8.274	17.59	19.77
420 nm	2.232	4.056	10.55	15.73
450 nm	1.776	3.413	8.770	14.23
475 nm	0.957	1.730	4.234	7.270
520 nm	0.598	1.057	2.412	3.823
600 nm	0.301	0.542	1.263	1.915
700 nm	0.052	0.108	0.272	0.416
808 nm	0.014	0.023	0.051	0.092
940 nm	0.012	0.015	0.019	0.036

Table S4 Photoresponsivity (unit: μA W^{-1}) of the as-fabricated $Pb_{0.50}Cd_{0.50}S$ QDs under SL and lasers with different wavenumbers at 0.4 V in 0.1 M KOH.

	Level I	Level II	Level III	Level IV
SL	368.4	591.2	433.3	297.4
380 nm	27310	**27580**	20690	13180
420 nm	5580	6760	5550	5070
450 nm	602.0	513.2	404.1	374.5
475 nm	333.4	290.8	189.0	185.0
520 nm	186.9	147.8	104.0	95.10
600 nm	96.69	86.03	62.52	54.56
700 nm	11.02	10.49	8.218	7.247
808 nm	5.785	4.466	3.091	3.239
940 nm	9.756	6.667	5.263	7.860

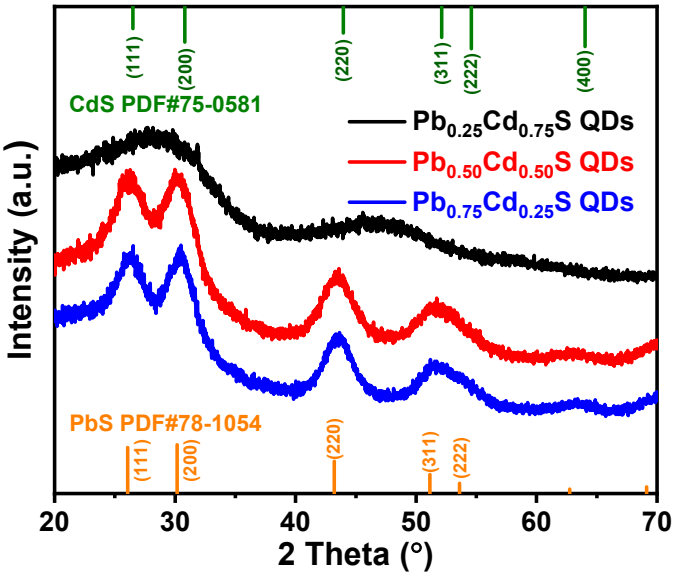

Fig. S1. XRD patterns of the $Pb_{1-x}Cd_xS$ QDs with different x.

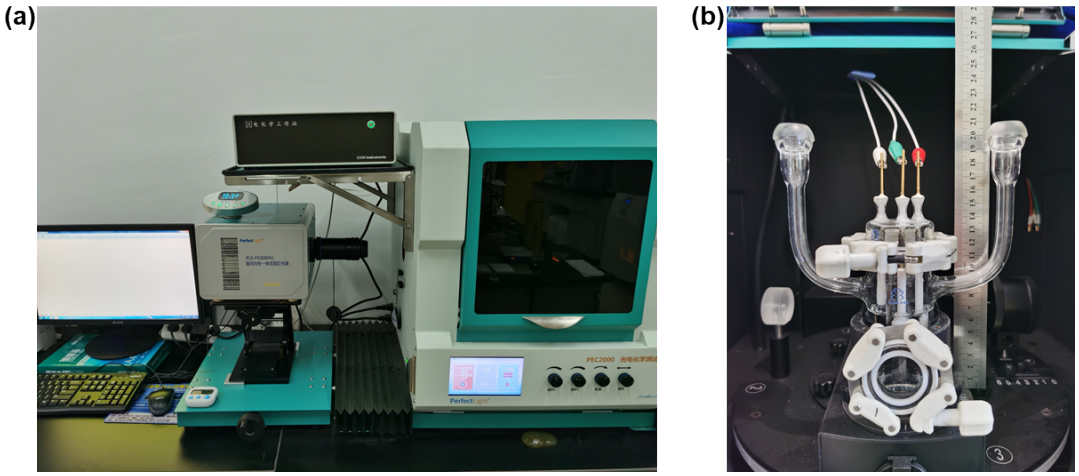

Fig. S2. Photographs of the (a) PEC measurement system and (b) standard three electrodes in the PEC system.

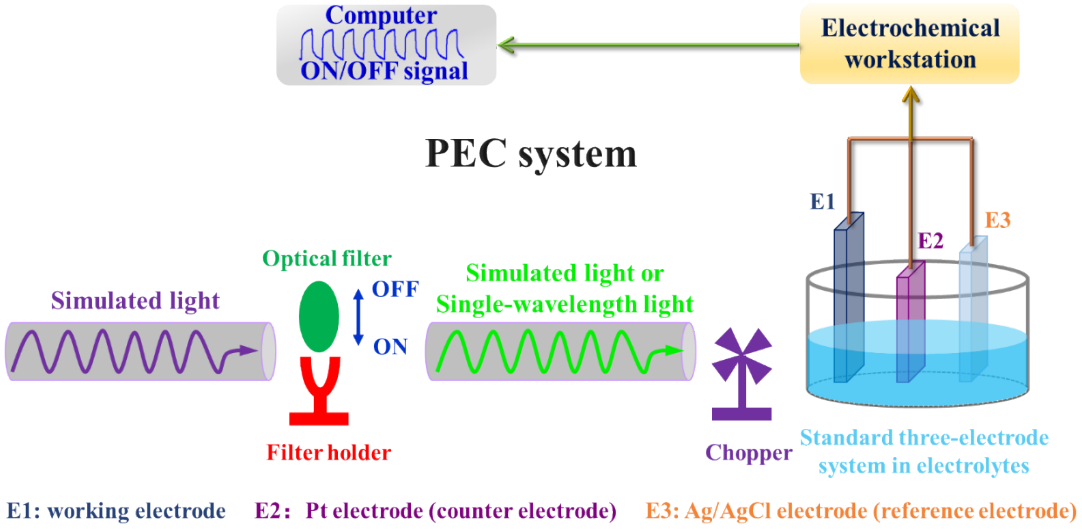

Fig. S3. The schematic illustration of the PEC measurement system.

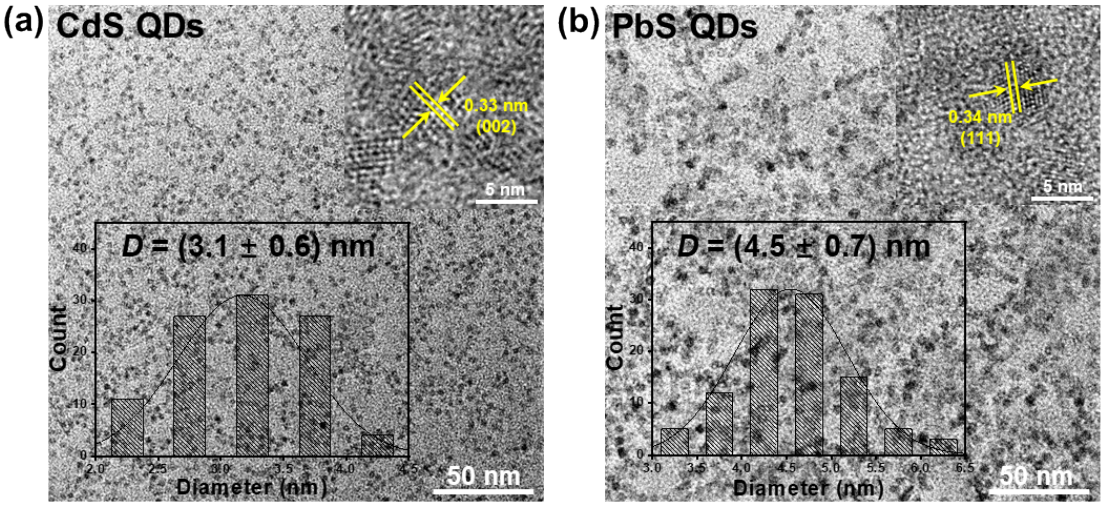

Fig. S4. TEM images of the (a) CdS QDs and (b) PbS QDs.

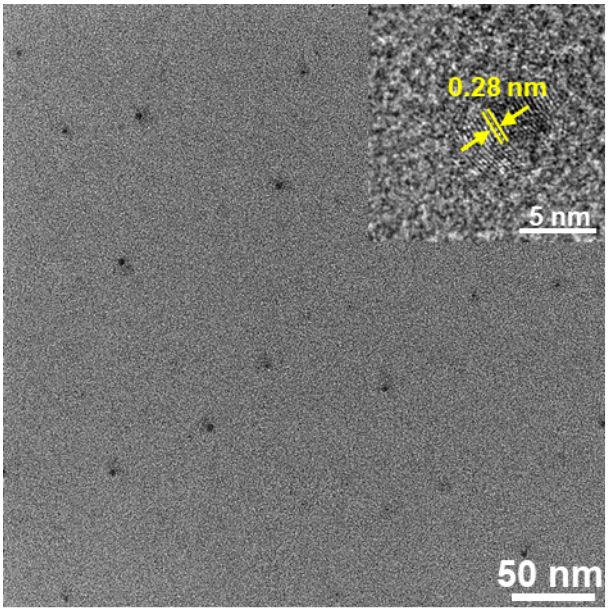

Fig. S5. TEM image of the $Pb_{0.50}Cd_{0.50}O$ bimetallic cluster; inset shows the HRTEM image.

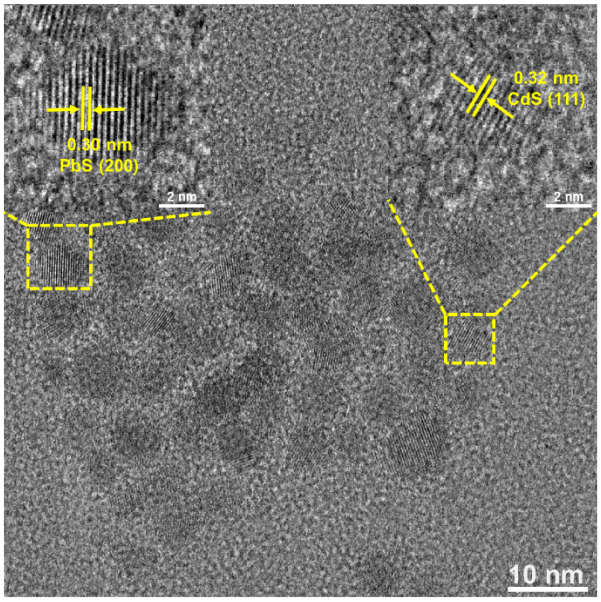

Fig. S6. TEM image of the $PbS_{0.50}/CdS_{0.50}$ QDs; insets show the corresponding HRTEM images of PbS QDs (upper left) and CdS QDs (upper right), respectively.

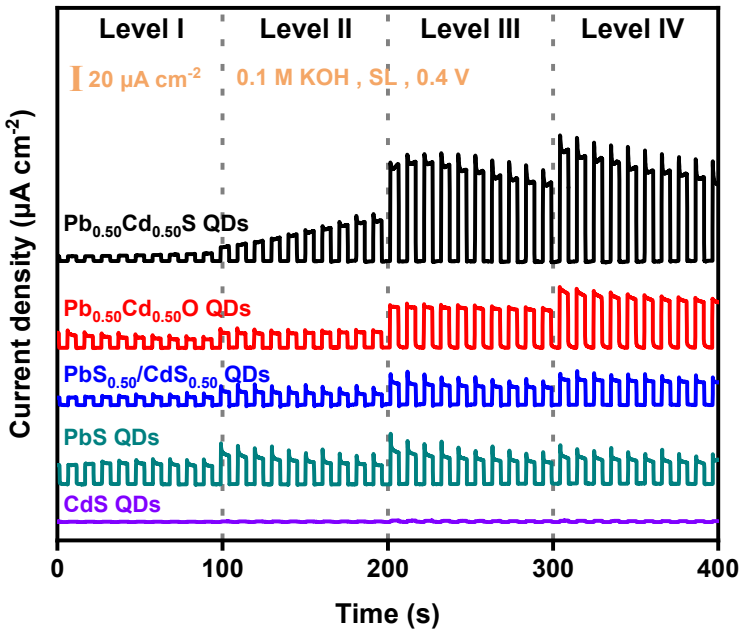

Fig. S7. The photoresponse behavior for different PEC electrodes in 0.1 M KOH at 0.4 V.

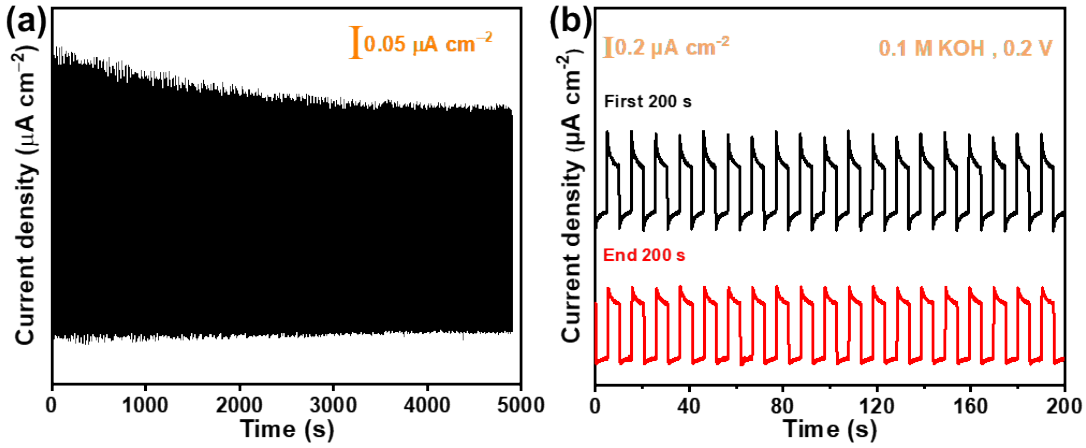

Fig. S8. (a) Photoresponse stability of the $Pb_{0.50}Cd_{0.50}S$ QD-based PEC electrode; and (b) enlarged areas for the first 200 s and end 200 s.

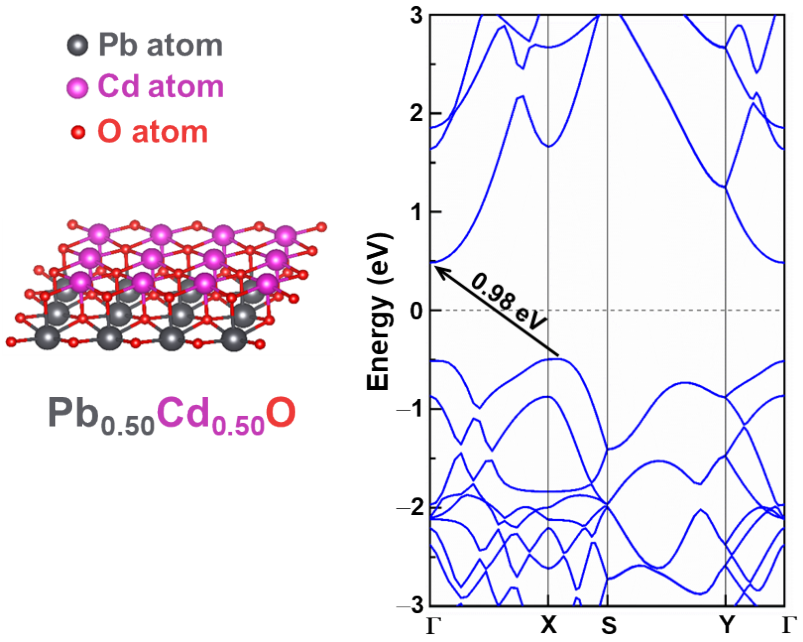

Fig. S9. Crystal structures of $Pb_{0.50}Cd_{0.50}O$ and its electronic band structure.